Development/Plasticity/Repair

FGF8 Signaling Regulates Growth of Midbrain Dopaminergic Axons by Inducing Semaphorin 3F

Kenta Yamauchi,[1]* Shigeki Mizushima,[1]* Atsushi Tamada,[2] Nobuhiko Yamamoto,[1] Seiji Takashima,[3] and Fujio Murakami[1,2]

[1]Laboratory of Neuroscience, Graduate School of Frontier Biosciences, Osaka University, Suita 565-0871, Japan, [2]Division of Behavior and Neurobiology, National Institute for Basic Biology, Okazaki 444-8585, Japan, and [3]Department of Molecular Cardiology, Osaka University Graduate School of Medicine, Suita 565-0871, Japan

Accumulating evidence indicates that signaling centers controlling the dorsoventral (DV) polarization of the neural tube, the roof plate and the floor plate, play crucial roles in axon guidance along the DV axis. However, the role of signaling centers regulating the rostrocaudal (RC) polarization of the neural tube in axon guidance along the RC axis remains unknown. Here, we show that a signaling center located at the midbrain–hindbrain boundary (MHB) regulates the rostrally directed growth of axons from midbrain dopaminergic neurons (mDANs). We found that beads soaked with fibroblast growth factor 8 (FGF8), a signaling molecule that mediates patterning activities of the MHB, repelled mDAN axons that extended through the diencephalon. This repulsion may be mediated by *semaphorin 3F* (*sema3F*) because (1) FGF8-soaked beads induced an increase in expression of *sema3F*, (2) *sema3F* expression in the midbrain was essentially abolished by the application of an FGF receptor tyrosine kinase inhibitor, and (3) mDAN axonal growth was also inhibited by sema3F. Furthermore, mDAN axons expressed a sema3F receptor, neuropilin-2 (nrp2), and the removal of *nrp-2* by gene targeting caused caudal growth of mDAN axons. These results indicate that the MHB signaling center regulates the growth polarity of mDAN axons along the RC axis by inducing sema3F.

Introduction

During development, growth cones navigate toward their targets by responding to cues in the extracellular milieu (for review, see Tessier-Lavigne and Goodman, 1996; Yu and Bargmann, 2001; Dickson, 2002; Huber et al., 2003). For axons to reach their correct targets, their growth directions must be precisely regulated. Because axonal growth in the neural tube occurs mainly in the rostrocaudal (RC) and dorsoventral (DV) directions, a fundamental question in neural development is how the polarized growth of axons along the RC and DV axes is achieved.

Accumulating evidence indicates that the roof plate and the floor plate play crucial roles in axon guidance along the DV axis (for review, see Colamarino and Tessier-Lavigne, 1995; Murakami and Shirasaki, 1997). In the spinal cord, for example, the repellent activities of the roof plate mediated by bone morphogenetic proteins (BMPs) (Augsburger et al., 1999; Butler and Dodd, 2003) and the attractive activities of the floor plate mediated by netrin-1 and sonic hedgehog (SHH) (Kennedy et al., 1994; Serafini et al., 1994, 1996; Charron et al., 2003) guide the axons of dorsally located commissural neurons toward the ventral midline. The floor plate causes changes in the growth cone's responsiveness to midline guidance cues, allowing commissural axons to cross the ventral midline (Shirasaki et al., 1998; Zou et al., 2000; Shirasaki and Murakami, 2001; Gore et al., 2008). Because both the roof plate and the floor plate act as signaling centers regulating the DV polarization of the neural tube (for review, see Tanabe and Jessell, 1996; Lee and Jessell, 1999; Jessell, 2000; Briscoe and Ericson, 2001; Caspary and Anderson, 2003; Chizhikov and Millen, 2005; Lupo et al., 2006), an intriguing question is whether signaling centers regulating the RC polarization of the neural tube also contribute to axon guidance along the RC axis.

To address this question, we focused on the midbrain–hindbrain boundary (MHB), a signaling center that regulates the RC polarity of the midbrain and rostral hindbrain (for review, see Liu and Joyner, 2001a; Wurst and Bally-Cuif, 2001; Raible and Brand, 2004; Nakamura et al., 2005). We selected axons from midbrain dopaminergic neurons (mDANs) as potential candidate neurons that are under the influence of the MHB because (1) these neurons arise near the ventral midline rostral to the MHB (for review, see Hynes and Rosenthal, 1999; Ang, 2006; Prakash and Wurst, 2006; Abeliovich and Hammond, 2007; Smidt and Burbach,

Received Oct. 6, 2008; revised Jan. 28, 2009; accepted Feb. 11, 2009.

This work was supported by Solution Oriented Research for Science and Technology from the Japan Science and Technology Agency and grants-in-aid from the Japan Society for the Promotion of Science and Ministry of Education, Culture, Sports, Science, and Technology of Japan. We thank Dr. Y. Tashiro for help in whole-embryo culture; Drs. K. Muguruma, Y. Zhu, and R. Shirasaki for technical advice; Dr. J. Miyazaki for a *pCAGGs* vector; Dr. G. Martin for a *Fgf8* plasmid; Dr. Y. Tanabe for a *pCAGGs-Fgf8b* plasmid; Dr. Y. Hatanaka for a *pCAGGs-EGFP* plasmid; Dr. D. Kawauchi for *Wnt-1* plasmids; and M. Torigoe for technical assistance. We also thank Drs. Y. Tanabe, Y. Zhu, D.-H. Tanaka, and R. Shirasaki for critical reading of this manuscript and Dr. P. Karagiannis for proofreading.

*K.Y. and S.M. contributed equally to this work.

Correspondence should be addressed to Fujio Murakami, Laboratory of Neuroscience, Graduate School of Frontier Biosciences, Osaka University, Suita 565-0871, Japan. E-mail: murakami@fbs.osaka-u.ac.jp.

S. Mizushima's present address: Fuji Oil Co., Ltd., Izumisano 598-8540, Japan.

A. Tamada's present address: Laboratory for Neuronal Growth Mechanisms, Brain Science Institute, RIKEN, Wako 351-0198, Japan.

N. Yamamoto's present address: Laboratory of Cellular and Molecular Neurobiology, Graduate School of Frontier Biosciences, Osaka University, Suita 565-0871, Japan.

DOI:10.1523/JNEUROSCI.4794-08.2009

 0270-6474/09/294044-12$15.00/0

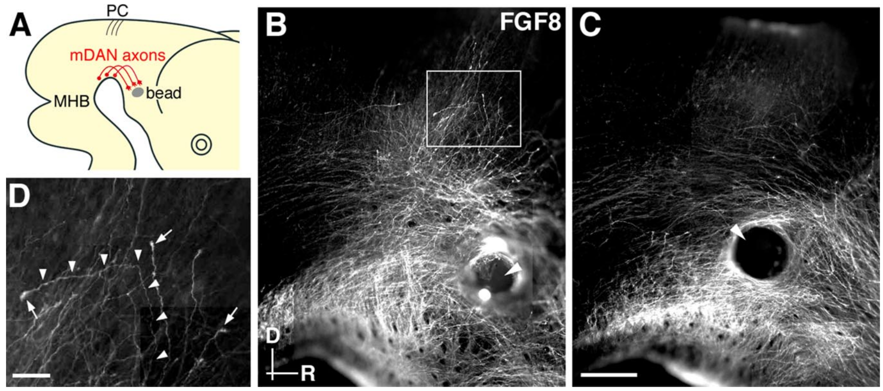

Figure 1. Ectopically expressed FGF8 disorganizes the rostrally directed growth of mDAN axons. ***A***, Schematic diagram showing the position of FGF8-bead implantation. FGF8-beads are embedded into the mDAN axonal pathway in the diencephalon. PC, Posterior commissure. ***B***, ***C***, mDAN axonal growth in an experimental (***B***) and a control (***C***) brain 2 d after bead placement. TH-positive axons were deflected dorsally in an FGF8-bead implanted brain. In contrast, in a BSA-bead-implanted brain, TH-positive axons grew rostrally ignoring the bead. White arrowheads show the position of beads, which were removed during the fixation procedure. D, Dorsal; R, rostral. ***D***, A higher-magnification image of the boxed area in ***B***. A caudally deflected mDAN axon is labeled by arrowheads. Growth cone-like structures were observed at the tip of axons (arrows). Scale bars: ***B***, ***C***, 200 μm; ***D***, 50 μm.

2007), (2) mDANs extend their axons rostrally to innervate the diencephalic and telencephalic targets (Lindvall and Björklund, 1983), and (3) the growth polarity of these axons is regulated by a substrate-associated cue(s) polarized along the RC axis in the midbrain (S. Nakamura et al., 2000).

In this study, we found that the trajectories of mDAN axons were perturbed *in vitro* by misexpression of fibroblast growth factor 8 (FGF8), a secreted molecule that can mimic patterning activities of the MHB (for review, see Liu and Joyner, 2001a; Wurst and Bally-Cuif, 2001; Raible and Brand, 2004; Nakamura et al., 2005). Furthermore, FGF8 induced the expression of an axon guidance molecule, *semaphorin 3F* (*sema3F*), in the midbrain/diencephalons, and the *sema3F* expression was markedly reduced by an FGF receptor tyrosine kinase inhibitor. These results suggest that sema3F guides mDAN axons as a downstream molecule of FGF8. Indeed, mDANs expressed the sema3F ligand-binding receptor neuropilin-2 (nrp2), and mDAN axon growth was inhibited by sema3F *in vitro*. Consistent with these observations, the removal of *nrp2* by gene targeting caused some mDAN axons to aberrantly grow caudally. Collectively, these findings suggest that FGF8 derived from the MHB controls the rostrally directed growth of mDAN axons by inducing sema3F. Part of this study has been reported in preliminary forms (Yamauchi et al., 2004, 2007).

Materials and Methods

Animals. Wistar rats (CLEA Japan or Nihon SLC) and *nrp2*-knock-out mice were used. Noon on the day of vaginal plug formation was designated as embryonic day 0.5 (E0.5), and the day of birth was designated as postnatal day 0 (P0). The generation of the $nrp2^{lacZ/lacZ}$ mice has been described previously (Takashima et al., 2002). All experiments followed the Osaka University *Guidelines for the Welfare and Use of Laboratory Animals*.

Expression vectors. To generate a *pCAGGs-myc* vector, *myc* epitope tag was ligated into an expression vector, *pCAGGs* (a gift from Dr. J. Miyazaki, Osaka University) (Niwa et al., 1991). A *pCAGGs-sema3F-myc* vector was prepared by subcloning the coding sequence of mouse *sema3F* into the *pCAGGs-myc* vector. The *sema3F*-coding sequence was obtained by PCR from E14.5 mouse brain cDNA. A *pCAGGs-enhanced green fluorescent protein (EGFP)* vector (Hatanaka and Murakami, 2002) was a gift from Dr. Y. Hatanaka (Nara Institute of Science and Technology, Nara, Japan); a CAG promoter-driven *Fgf8b* (Tanaka et al., 1992) expression vector, *pCAGGs-Fgf8b*, was a gift from Dr. Y. Tanabe (Osaka University); and a *pCAGGs-Wnt-1-myc* vector was a gift from Dr. D. Kawauchi (Chiba University, Chiba, Japan).

Expression of sema3F in COS-7 cells. COS-7 cells were maintained in DMEM (Nissui) containing 10% fetal bovine serum, 600 mg/L L-glutamine, and 1% penicillin/streptomycin (Nacalai Tesque). The *pCAGGs-sema3F-myc* vector was transfected into the COS-7 cells with FuGENE6 (Roche Diagnostics) according to the manufacturer's instructions. Aggregates of COS-7 cells were prepared using the hanging drop method (Shirasaki et al., 1995). The *pCAGGs-myc* vector was used as a control vector.

Culture. For whole-embryo culture, E9.5 or E11.5–E12 rat embryos were prepared by standard dissection techniques (Osumi and Inoue, 2001). In brief, dissections were performed in Tyrode's saline buffer at 37°C within 1 h of uterus collection. The decidual masses were dissected from the uteri, and the decidual layers and Reichert's membrane were removed, leaving the placenta intact. At E11.5–E12, a slit was made in the yolk sac and the amnion membrane to expose the embryo to the oxygenated medium. The embryos were then placed into small roller bottles of a whole-embryo culture apparatus (RKI10-0310; Ikemoto). Each bottle was filled with a 50% rat serum in DMEM/F-12 (D-8900; Sigma), supplemented with 3.85 g/L D-glucose, 2 mM L-glutamine, and 1% penicillin/streptomycin (Nacalai Tesque) (hereafter called DMEM/F-12) (Shirasaki et al., 1996). The bottles were then placed on the rotator of the culture apparatus at 37°C for 1–3 d. Oxygen was supplied to the embryos according to Osumi and Inoue (2001).

To analyze the effects of FGF8 on axonal growth and molecular expression in *in vivo*-like conditions, FGF8-soaked beads (FGF8-beads) were implanted onto the growth pathways of mDAN axons in whole-embryo culture preparations (see Fig. 1*A*). FGF8-beads were prepared according to Liu et al. (1999). In brief, heparinized acrylic beads (H5263; Sigma) were immersed in FGF8b (1 mg/ml; R & D Systems) containing PBS for at least 3 h at room temperature. Bovine serum albumin (BSA) solution (50 mg/ml in PBS; Sigma) was used as a control. The embryos were placed on a rotator at 37°C for 0.5–1 h before bead transplantation. For bead implantation, a small incision was made with a glass needle in the ventral diencephalon. Then, the beads were washed with PBS and pushed into the ventral diencephalon using forceps. The embryos were returned to the roller-bottles and cultured.

To block FGF signaling in whole-embryo culture, an FGF receptor tyrosine kinase inhibitor, SU5402 (100 μM; Calbiochem) (Mohammadi et al., 1997), was added to the culture medium at the onset of the culture. Dimethylsulfoxide (DMSO), the vehicle for SU5402, was used in controls.

To examine the effect of FGF8 and sema3F on mDAN axonal growth, ventrorostral midbrain (VRM) explants were cultured as described previously (S. Nakamura et al., 2000), with some modifications. Briefly, VRM explants containing mDANs were dissected from E13.5 rat embryos. The explants and FGF8-beads or sema3F-expressing COS-7 cell aggregates were embedded in collagen gels at a distance of 300–1000 μm and cultured in DMEM/F-12 supplemented with 1% N_2 supplement (Invitrogen). The cultures were incubated in a 5% CO_2, 95% humidity incubator at 37°C for 2 d.

Electroporation. DNA constructs were introduced into rat embryos by electroporation as described previously (Osumi and Inoue, 2001). After a 1–2 h preincubation on a rotator at 37°C, each embryo was transferred into a Petri dish containing Tyrode's saline buffer. DNA solutions (1.5 mg/ml in PBS with 0.01% Fast Green) were pressure-injected into the third ventricle of the embryo with a glass micropipette fitted to an injector (IM-30; Narishige). Electroporation was performed using tweezer-type electrodes with 2-mm-diameter discs (CUY6502; Unique Medical). Electric pulses of 10 or 15 V were charged four times for 50 ms at 950 ms intervals using a square-pulse generator (CUY21, Nepa Gene Company; or ECM830, BTX). The electroporated embryo was rinsed with Tyrode's saline buffer and returned to the culture apparatus.

In situ *hybridization.* To prepare RNA probes for *in situ* hybridization, the following plasmid templates were used. A plasmid containing *Fgf8* was a gift from Dr. G. Martin (University of California, San Francisco, San Francisco, CA), and a plasmid used to generate *Wnt-1* riboprobe was a gift from Dr. D. Kawauchi (Chiba University). Partial cDNA fragments of *sema3A* (base pairs 1688–2248, GenBank accession number X95286), *sema3B* (base pairs 2153–2653, GenBank accession number X85990), *sema3C* (base pairs 94–637, GenBank accession number X85994), *sema3D* (base pairs 89–750, GenBank accession number AF268594), *sema3E* (base pairs 1906–2645, GenBank accession number AF034744), *sema3F* (base pairs 596–1300, GenBank accession number AF080090), *sema3G* (base pairs 1457–2196, GenBank accession number NM_001025379), *nrp2* (base pairs 1337–1898, GenBank accession number AF016297), *orthodenticle homolog 2* (*otx2*) (base pairs 222–1073, GenBank accession number NM_144841), and *engrailed-2* (*en-2*) (base pairs 23–1082, GenBank accession number NM_010134) were amplified by PCR from rat or mouse brain cDNA. The coding sequence of *EGFP* was prepared by PCR amplification from the *pCAGGs-EGFP* vector. The resulting fragments were subcloned into the pGEM-T vector or the pGEM-T Easy vector (Promega) for subsequent riboprobe preparation. The antisense and sense riboprobes were transcribed *in vitro* using digoxigenin (DIG) or fluorescein isothiocyanate (FITC)-UTP (Roche Diagnostics).

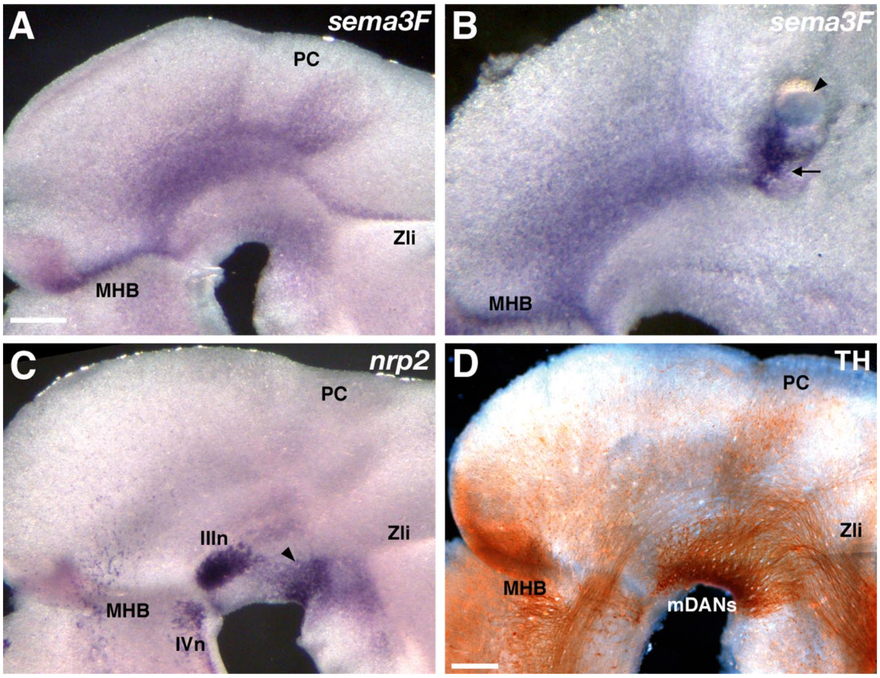

Figure 2. Expression pattern of *sema3F* and its induction by FGF8-beads in whole-embryo culture. ***A***, The distribution of sema3F transcripts in rat midbrain at E13.5. ***B***, *sema3F* expression in a midbrain preparation 2 d after an FGF8-bead (arrowhead) implantation. Sema3F transcripts were induced in the region just ventral to the bead (arrow). ***C***, The distribution of nrp2 mRNAs in an E13.5 rat midbrain. Nrp2 mRNAs were observed in the rostral region of the ventral most midbrain (arrowhead). *nrp2* was also detected in the IIIn and IVn. ***D***, An E13.5 rat midbrain hemisphere immunostained for TH. mDAN axons appear to avoid the *sema3F*-expressing region (compare ***A***, ***D***). PC, Posterior commissure; Zli, zona limitans intrathalamica; IIIn, oculomotor nucleus; IVn, trochlear nucleus. Scale bars: ***A***, ***C***, ***D***, 300 μm; ***B***, 375 μm.

In situ hybridization of whole-mount preparations was performed as described previously (Bally-Cuif et al., 1992). In brief, tissues were fixed with 4% paraformaldehyde (PFA) in 0.12 M phosphate buffer (PB) and dehydrated in an ascending series of methanol. After rehydration in a descending methanol series, the tissues were treated with 10 μg/ml proteinase K and hybridized with 1.0 μg/ml RNA probes for 16 h at 60 or 70°C. After RNase digestion and high-stringency washes, the samples were reacted with an alkaline phosphatase-conjugated anti-DIG antibody (1:2000; Roche Diagnostics). The signal was detected by subsequent reaction with nitroblue tetrazolium (NBT)/5-bromo-4-chloro-3-indolyl phosphate (BCIP) (Roche Diagnostics).

Two-color *in situ* hybridization was performed as described previously (Dietrich et al., 1997), with some modifications. The tissues were hybridized simultaneously with DIG- and FITC-labeled antisense riboprobes for 16 h at 70°C. The DIG-labeled probes were first detected with NBT/BCIP (Roche Diagnostics). After the first color development, alkaline phosphatase was inactivated by incubation at 70°C for 30 min. The tissues were incubated overnight at 4°C with an alkaline phosphatase-conjugated anti-FITC antibody (1:2000; Roche Diagnostics) and visualized by 2,4-iodophenyl-3,4-nitrophenyl tetrazolium chloride/BCIP (Roche Diagnostics).

Immunohistochemistry. The whole-mount preparations were immunostained as described previously (S. Nakamura et al., 2000). The primary antibodies used were a rabbit polyclonal anti-tyrosine hydroxylase (TH) antibody (1:250; Millipore Bioscience Research Reagents) and a rabbit polyclonal anti-β-galactosidase (β-gal) antibody (1:10,000; ICN Biomedicals). After incubation with the primary antibodies, the preparations were incubated with a cyanine 3 (Cy3)-conjugated anti-rabbit IgG (1:100; Jackson ImmunoResearch) or a biotinylated anti-rabbit IgG (1:200; Vector Laboratories), then with Cy3-conjugated streptavidin (1:500; Jackson ImmunoResearch) or an avidin–biotin peroxidase complex (Vectastain ABC Elite kit; Vector Laboratories). Color was developed in 0.05% diaminobenzidine tetrahydrochloride and 0.005% H_2O_2 in Tris-buffered saline. All antibodies were diluted in PBS with 1% normal goat or horse serum (Vector Laboratories) and 1% Triton X-100.

For tissue sections, fresh brains were immediately immersed in 4% PFA in 0.12 M PB at 4°C from 90 min to overnight. The PFA-fixed brains were cryoprotected by immersion in 30% sucrose in 0.1 M PB, embedded in OCT compound (Sakura Finetechnical), and quickly frozen. Then, 20- to 50-μm-thick coronal or sagittal sections were cut on a cryostat (HM500; Zeiss), mounted on slides (Superfrost Plus; Thermo Fisher Scientific), and subjected to immunohistochemistry. The primary antibodies used were as follows: a rabbit polyclonal anti-nrp2 antibody (1:250), a rabbit polyclonal anti-TH antibody (1:250; Millipore Bioscience Research Reagents), a sheep polyclonal anti-TH antibody (1:100; Millipore Bioscience Research Reagents), a rat monoclonal anti-dopamine transporter (DAT; Slc6a3; Mouse Genome Informatics) antibody (1:1000; Millipore Bioscience Research Reagents), and a rabbit polyclonal anti-β-gal antibody (1:5000; ICN Biomedicals). The procedures for the anti-nrp2 antibody production followed those of anti-Robo antibodies (Tamada et al., 2008). The specificity of the anti-nrp2 antibody was confirmed by immunostaining with antibodies preabsorbed with a nrp2 ectodomain-Fc fusion protein or Fc protein and examination of immunoreactivities in *nrp2*-knock-out mice preparations. The secondary antibodies were a Cy3-conjugated anti-rabbit IgG (1:400; Jackson ImmunoResearch), an Alexa Fluor 488-conjugated anti-rat IgG (1:300; Invitrogen), an Alexa Fluor 594-conjugated anti-rabbit IgG (1:1000; Invitrogen), and a biotinylated anti-sheep IgG (1:500; Jackson ImmunoResearch). Cy2-conjugated streptavidin (1:600; Jackson ImmunoResearch) was used for visualization. All the procedures were the same as those used for whole-mount preparations, except that Triton X-100 in the antibody solutions was reduced to 0.05 or 0.2%. In double-labeling experiments, the sections were sequentially incubated with primary and secondary antibodies. Stained sections were observed with an epiflu-

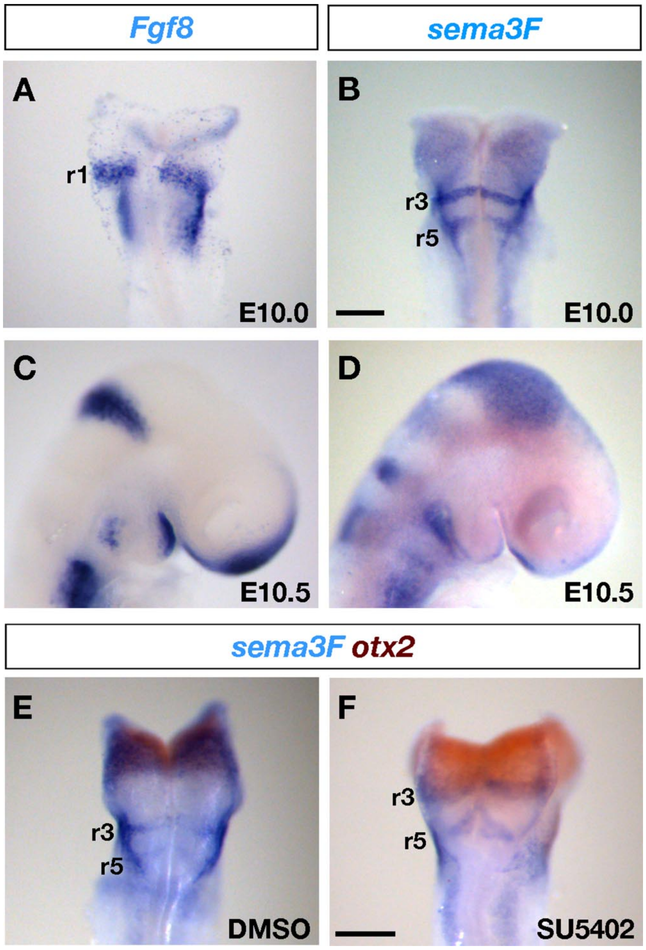

Figure 3. FGF signaling is required for *sema3F* expression in the midbrain. ***A–D***, Whole-mount *in situ* hybridization with *Fgf8* (***A***, ***C***) and *sema3F* (***B***, ***D***) antisense riboprobes in E10.0 (***A***, ***B***) and E10.5 (***C***, ***D***) rat embryos. Expression of *Fgf8* temporally preceded *sema3F* at the MHB. ***E***, ***F***, The distribution of *sema3F* (blue) and *otx2* (brown) in a DMSO-treated (***E***) and a SU5402-treated (***F***) embryo. The colocalization of *sema3F* (blue) and *otx2* (brown) was observed in a control embryo (***E***). In contrast, sema3F mRNAs in the *otx2*-positive region was nearly undetectable in a SU5402-treated embryo (***F***). *sema3F* expressions in the hindbrain were not affected by the application of SU5402. Scale bars: 200 μm.

orescence microscope (BX60; Olympus) or a confocal microscope (TCS SP2 AOBS; Leica Microsystems).

Quantitative analysis. To assess the defasciculation of TH-positive axons, images of TH-immunostained midbrains were captured by a confocal microscope (MRC-1024; Bio-Rad) at a depth of 0–75 μm below the surface of the preparation. The five most dorsally running axons were then selected in each individual animal. From each of the five, a line was drawn perpendicular to the ventral midline. The average length of the five lines was designated as the width of the TH-positive axonal bundle in the preparation.

To quantify the effect of sema3F on mDAN neurite outgrowth, TH-stained explants were photographed and digitized with an epifluorescence microscope (BX60; Olympus) equipped with a CCD camera (AxioCam; Zeiss). The image was thresholded, and the number of pixels of neurites was counted in the proximal and distal quadrants (see Fig. 5*C*) (Wang et al., 1996; de Castro et al., 1999) using NIH Image version 1.63. The central regions of the explants, occupied by cell soma, were excluded from the analysis. The number of pixels was then divided by the perimeter of the explant. This was designated as the "neurite outgrowth index." The Mann–Whitney *U* test was used in each analysis.

Results

Disruption of mDAN axon growth by ectopically expressed FGF8

We explored whether MHB activities are involved in the rostrally directed growth of mDAN axons. For this, the influence of ectopically expressed FGF8, a signaling molecule that mediates patterning activities of the MHB (for review, see Liu and Joyner, 2001a; Wurst and Bally-Cuif, 2001; Raible and Brand, 2004; Nakamura et al., 2005), on mDAN axonal growth was examined. Rat embryos were dissected at E11.5–E12, before mDANs initiate axonal growth ($n = 7$) (supplemental Fig. 1*A*, available at www.jneurosci.org as supplemental material) (S. Nakamura et al., 2000), and subjected to whole-embryo culture. FGF8-beads were implanted into the mDAN axonal pathway in the diencephalon at the beginning of the culture (Fig. 1*A*). We first confirmed whether FGF8-beads were able to mimic MHB activities with *in situ* hybridization for *en-2*, an early marker of midbrain development (Davis et al., 1988). In agreement with previous studies (Crossley et al., 1996; Liu et al., 1999; Martinez et al., 1999; Shamim et al., 1999; Liu and Joyner, 2001b), en-2 transcripts were detected around the FGF8-beads, 2 d after implantation ($n = 4$ of 4) (supplemental Fig. 2*A*, available at www.jneurosci.org as supplemental material). In contrast, no expression was found in the region where BSA-soaked beads (BSA-beads) were implanted ($n = 4$ of 4) (supplemental Fig. 2*B*, available at www.jneurosci.org as supplemental material). These findings suggest that FGF8-beads can mimic MHB activities. We next examined the effect of ectopically expressed FGF8 on mDAN axonal growth. After a 2–3 d culture, mDAN axons were visualized by immunostaining with an antibody directed against TH, the rate-limiting enzyme of dopamine synthesis. In the absence of the beads, TH-positive axons originating from the ventral midbrain traveled rostrally during the culture period, similarly to the projection *in vivo* ($n = 18$ of 18) (supplemental Fig. 1*B*,*C*, available at www.jneurosci.org as supplemental material). However, when an FGF8-bead was implanted into the mDAN axon pathway, the growth of the mDAN axons was perturbed substantially (Fig. 1*B*). Although a fraction of these axons appeared to pass underneath the bead, a considerable number of axons were deflected dorsally ($n = 11$ of 12) (Fig. 1*B*). Some axons even directed caudally as if they were repelled by the beads ($n = 5$ of 12) (Fig. 1*D*). In contrast, in control cultures implanted with BSA-beads, mDAN axons elongated rostrally, ignoring the beads ($n = 6$ of 6) (Fig. 1*C*). These findings suggest that FGF8 signaling is involved in the guidance of mDAN axons.

Induction of *sema3F* by FGF8

Implantation of FGF8-beads repatterned surrounding tissue as indicated by *en-2* expression (supplemental Fig. 2*A*, available at www.jneurosci.org as supplemental material). This observation, together with the induced repulsion toward mDAN axons by implanted FGF8-beads (Fig. 1*B*), prompted us to test the possibility that FGF8-beads affect mDAN axonal growth by inducing a repellent molecule(s).

Because class 3 semaphorins (sema3A–sema3G) are repellent molecules that contribute widely to axon guidance (for review, see Yu and Bargmann, 2001; Dickson, 2002; Huber et al., 2003), class 3 semaphorins are potential candidates for such repellents downstream from FGF8. Therefore, we explored the mRNA expression of class 3 semaphorins in the midbrain (supplemental Fig. 3, available at www.jneurosci.org as supplemental material). Of the seven class 3 semaphorins, only sema3F transcripts were detected at the MHB at the stage of mDAN axon development

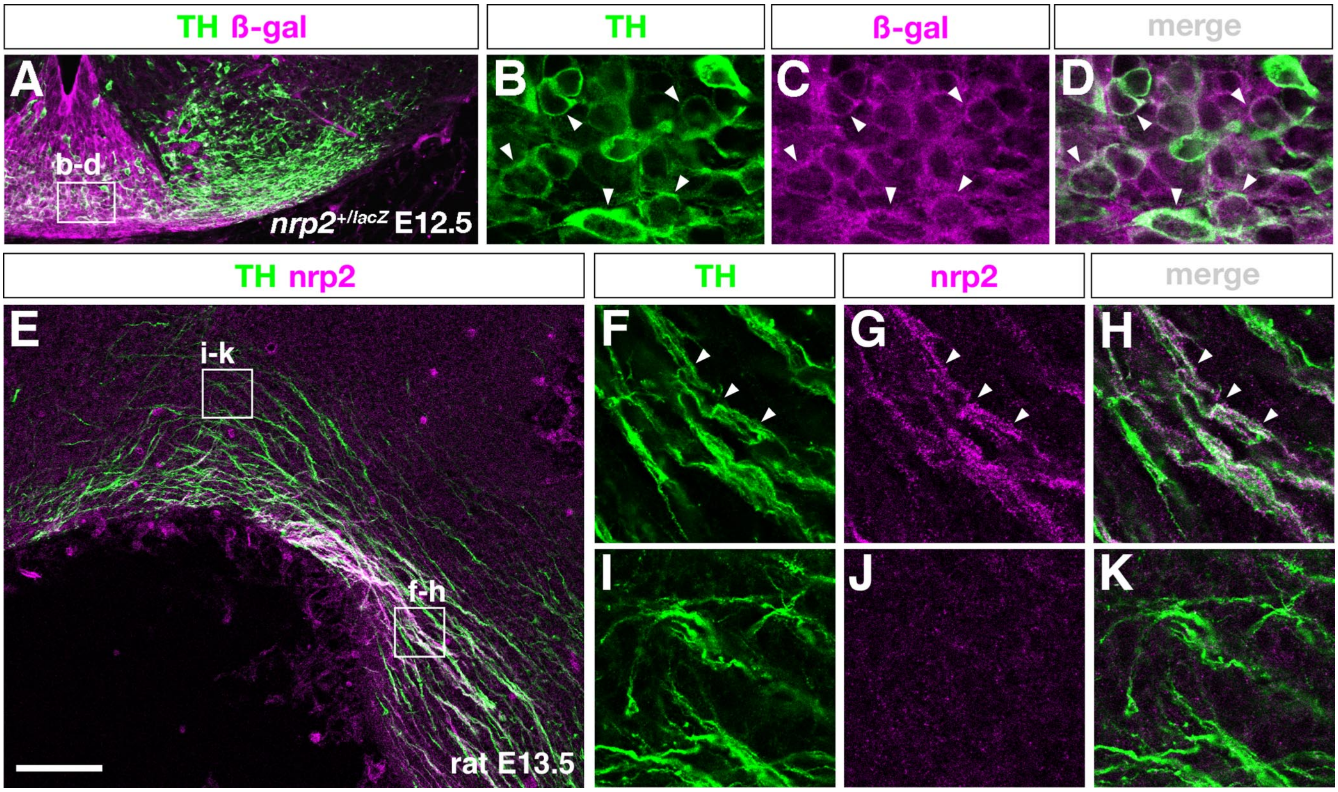

Figure 4. Nrp2 is expressed on a subset of mDAN axons. ***A***, A midbrain coronal section of E12.5 *nrp2*$^{+/lacZ}$ midbrain immunostained for TH (green) and β-gal (magenta). ***B–D***, Higher-magnification views of the boxed area in ***A***. ***B***, ***C***, TH (***B***) and β-gal (***C***) expression. ***D***, A merged image of ***B*** and ***C***. β-gal immunoreactivity was observed in almost all TH-positive cells (arrowheads). ***E***, An E13.5 rat midbrain/diencephalon parasagittal section immunostained for TH (green) and nrp2 (magenta). ***F–K***, High-power views of the boxed areas (f–h, i–k) in ***E***. ***F***, ***G***, ***I***, ***J***, TH (***F***, ***I***) and nrp2 (***G***, ***J***) expression. ***H***, A merged view of ***F*** and ***G***. ***K***, A merged image of ***I*** and ***J***. The colocalization of TH and nrp2 was observed in the rostroventral region (***F–H***) but not in the dorsal region (***I–K***). Scale bar: ***A***, ***E***, 100 μm; ***B–D***, ***F–H***, ***I–K***, 20 μm.

($n = 8$) (Fig. 2*A*). The *sema3F* expression pattern was complementary to that of the mDAN axon trajectories ($n = 4$) (Fig. 2, compare *A*, *D*). We then examined whether FGF8 induces the expression of *sema3F* using whole-embryo culture preparations implanted with FGF8-beads. Sema3F mRNA was detected in the region surrounding the FGF8-beads after 2 d in culture ($n = 7$ of 8) (Fig. 2*B*). In contrast, no sema3F transcripts were induced by BSA-beads ($n = 5$ of 5) (data not shown). Together, these findings raise the possibility that FGF8 can induce *sema3F* expression in the midbrain. This notion was supported by an independent experiment using electroporation-based gene transfer. When a plasmid coding for *Fgf8b* was introduced into the midbrain followed by whole-embryo culture, *sema3F* was induced in the area surrounding the *Fgf8*-expression ($n = 9$ of 11) (supplemental Fig. 4*A*, available at www.jneurosci.org as supplemental material). In preparations electroporated with mock plasmid, the *sema3F* expression was unaffected ($n = 9$ of 9) (supplemental Fig. 4*B*, available at www.jneurosci.org as supplemental material).

We next explored whether *sema3F* is induced by FGF8 during embryonic development. If *sema3F* expression in the midbrain is induced by FGF8, one should expect that *sema3F* expression is preceded by the expression of *Fgf8*. As expected, whereas FGF8 mRNA was detected in rhombomere 1 (r1) from E10 (six-somite stage) (Fig. 3*A*, E10.0, $n = 5$, *C*, E10.5, $n = 4$), sema3F mRNA was first detected in the midbrain only at E10.5 (Fig. 3*B*, E10.0, $n = 6$, *D*, E10.5, $n = 4$). We next explored whether FGF signaling is required for *sema3F* expression in the midbrain. For this, rat embryos were subjected to whole-embryo culture in the presence or absence of the FGF receptor tyrosine kinase inhibitor SU5402 (Mohammadi et al., 1997) before the development of the *sema3F* expression in the midbrain (at E9.5 or zero- to two-somite stage). After a 27–30 h culture in control DMSO, the *sema3F* expression was clearly detected in the midbrain as indicated by *otx2* expression (Simeone et al., 1992, 1993) ($n = 11$ of 11) (Fig. 3*E*). However, in SU5402-treated embryos, the hybridization signal for *sema3F* in the *otx2*-positive region was nearly undetectable ($n = 19$ of 19) (Fig. 3*F*). These findings support the notion that the expression of *sema3F* in the midbrain was induced by FGF8 signaling emanating from the MHB, although a quantitative analysis might be necessary to confirm this notion.

Expression of nrp2 by mDAN axons

All class 3 semaphorins signal through a holoreceptor complex composed of a ligand-binding component and a signal-transducing component, except sema3E (for review, see F. Nakamura et al., 2000; Raper, 2000; Fujisawa, 2004; Kruger et al., 2005; Tran et al., 2007; Zhou et al., 2008). If sema3F contributes to mDAN axon guidance, its ligand-binding receptor, nrp2 (Chen et al., 1997, 1998; Kolodkin et al., 1997; Giger et al., 1998), should be expressed by these axons. Indeed, nrp2 mRNA was intensely expressed near the ventral midline region where mDANs are likely to be located ($n = 8$) (Fig. 2*C*, arrowhead).

To confirm nrp2 expression in mDANs, we next examined the colocalization of TH and β-gal in the ventral midbrain of E12.5 *nrp2* $^{+/lacZ}$ mice. In this mouse line, the bacterial *lacZ* gene is knocked into the *nrp2* locus (Takashima et al., 2002). As shown in Figure 4*A–D*, most TH-positive cells, in particular those near the ventral midline, highly expressed β-gal from the *nrp2* locus ($n =$

4), indicating nrp2 transcriptional activity in most mDANs. We then investigated nrp2 protein expression in mDAN axons with double immunohistochemical staining for TH and nrp2. We found that many mDAN axons coursing through the rostroventral midbrain expressed high-level nrp2 at E13.5 ($n = 8$) (Fig. 4*E–K*), although some dorsally coursing mDAN axons expressed no or low-level nrp2. Together, these results indicate that nrp2 is expressed at least on a subset of mDAN axons.

Sema3F inhibits mDAN axon outgrowth

The results above raise the possibility that sema3F/nrp2 signaling regulates mDAN axon growth. We performed *in vitro* coculture experiments to test this possibility. VRM explants, which contained nrp2-positive mDANs ($n = 9$ of 9) (supplemental Fig. 5, available at www.jneurosci.org as supplemental material), were dissected from E13.5 rat embryos and cocultured with aggregates of *sema3F*-transfected COS-7 cells in collagen gels. After 2 d, TH-positive neurites elongated almost symmetrically from the VRM explants in the cocultures with mock-transfected COS-7 cell aggregates (Fig. 5*A*). In contrast, in the cocultures with sema3F-expressing COS-7 cell aggregates, neurite outgrowth from VRM explants was dramatically reduced on the side facing the cell aggregates (Fig. 5*B*). The neurite outgrowth index in the quadrant proximal to the sema3F-expressing COS-7 cells was reduced to ~30% of that of the control (control: 1889 ± 413.7, $n = 22$; sema3F: 652.0 ± 126.8, $n = 27$; $p = 0.0013$, Mann–Whitney *U* test), whereas the index in the distal quadrant did not differ significantly between the two groups (control, 1564.97 ± 271.8; sema3F, 1161.32 ± 161.2; $p = 0.2959$, Mann–Whitney *U* test). We also found a significant decrease in the overall outgrowth of TH-positive neurites in the cocultures with sema3F-expressing COS-7 cell aggregates (control, 6342.8 ± 1194.85; sema3F, 3221.0 ± 424.31; $p = 0.0244$, Mann–Whitney *U* test). These results indicate that sema3F repels or inhibits mDAN axon outgrowth *in vitro*.

Caudally directed growth of mDAN axons in *nrp2*-knock-out mice

Sema3F mRNA was detected at the MHB, whereas mDAN axons extended rostrally in the ventral midbrain (Fig. 2, compare *A*, *D*). These findings raise the possibility that sema3F/nrp2 signaling contributes to the rostrally directed growth of mDAN axons. To explore this possibility, we first examined the RC polarity of mDAN axon growth in *nrp2*-knock-out mice. At E12.5, no notable difference in the RC growth polarity of mDAN axons was observed between $nrp2^{+/+}$ and $nrp2^{lacZ/lacZ}$ mice (data not shown). However, at E14.5, we noted a clear phenotypic difference. Whereas mDAN axons never extended caudally in wild-type animals ($n = 3$ of 3) (Fig. 6*A*,*C*), mDAN axon subsets in the *nrp2*-knock-out mice grew caudally and even invaded the rostral hindbrain ($n = 3$ of 3) (Fig. 6*B*,*C*). These aberrant TH-positive fibers were observed until P0, the oldest stage analyzed (Fig. 6*D*,*E*) ($nrp2^{+/+}$, $n = 3$ of 3; $nrp2^{lacZ/lacZ}$, $n = 3$ of 3), suggesting their persistence. Because TH is expressed not only by dopaminergic neurons but also by noradrenergic neurons, these aberrant axons could be noradrenergic axons originated from the locus ceruleus. To confirm that these TH-positive fibers were indeed mDAN axons, we performed a double-labeling study with antibodies against TH and DAT (Slc6a3; Mouse Genome Informatics), a molecule expressed in mDAN subsets but not in locus ceruleus neurons (Ciliax et al., 1995; Freed et al., 1995). We found that DAT was expressed in a subset of aberrant TH-positive fibers ($n = 5$ of 5) (Fig. 6*F–H*). Moreover, these mDAN axons expressed β-gal ($n = 3$ of 3) (Fig. 6*I–K*), suggesting that *nrp2*-expressing mDAN axons were deflected caudally in the *nrp2*-knock-out mice. The RC patterning in the midbrain seemed normally in *nrp2*-knock-out mice (supplemental Fig. 6, available at www.jneurosci.org as supplemental material). Together, these findings demonstrate that sema3F/nrp2 signaling controls the RC growth polarity of mDAN axons.

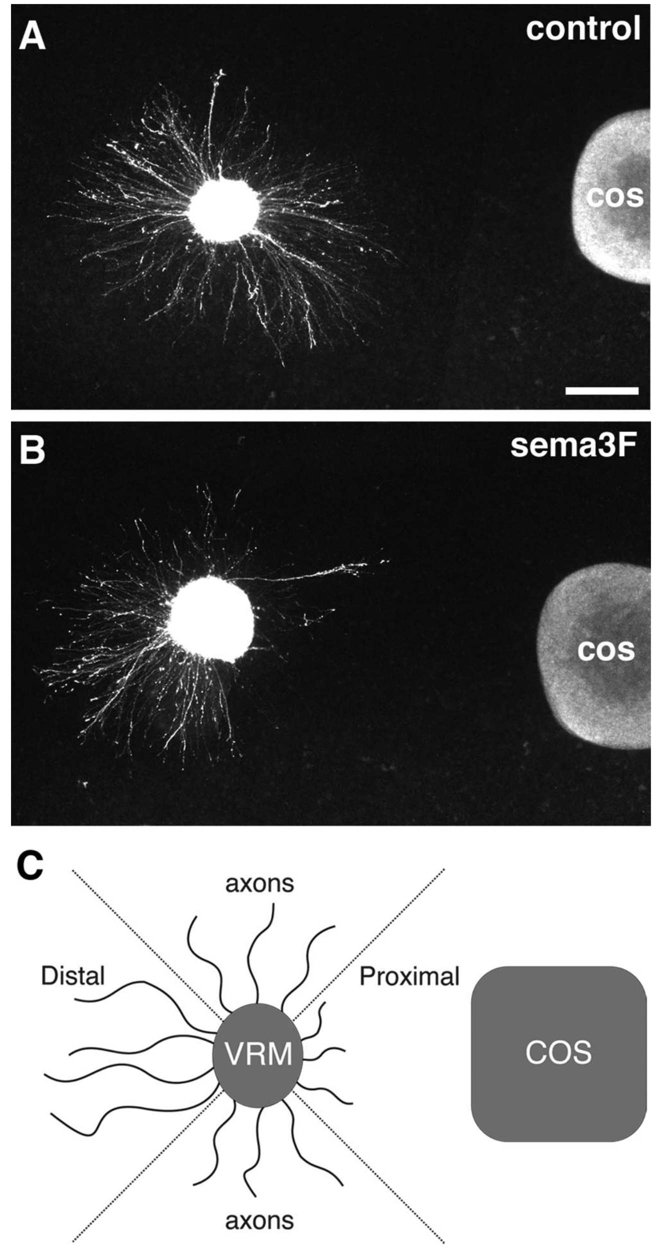

Figure 5. Sema3F inhibits the mDAN neurite outgrowth *in vitro*. ***A***, ***B***, VRM explants from E13.5 rat embryos were cocultured with aggregates of COS-7 cells transfected with either the *pCAGGs-myc* (***A***) or the *pCAGGs-sema3F-myc* (***B***) vector in collagen gels. After 2 d, the explants were fixed and stained with an anti-TH antibody. Neurite outgrowth from VRM explants, which is almost symmetric in a control coculture (***A***), appears to be inhibited by sema3F (***B***). ***C***, Scheme of the method used to quantify neurite outgrowth. Scale bar, 250 μm.

Dorsal spread of mDAN axons in *nrp2*-knock-out mice

Sema3F mRNA was detected not only at the MHB but also in the dorsal midbrain/diencephalon along the mDAN axonal trajectory (Fig. 2, compare *A*, *D*). Therefore, we next asked whether sema3F/nrp2 signaling is also involved in defining the dorsal border of mDAN axon trajectories. Whole-mount preparations of E12.5 embryos were stained with an anti-TH antibody to test this idea. In wild-type and *nrp2*$^{+/lacZ}$ mouse brains, mDAN axons grew rostrally, forming tightly fasciculated axonal bundles (n = 16 of 16) (Fig. 7*A*). In contrast, in *nrp2*-knock-out mice, these axonal bundles were less fasciculated, and a substantial number of mDAN axons grew more dorsally (n = 16 of 16) (Fig. 7*B*). The mDAN axonal bundles in *nrp2*-knock-out mice were significantly broader than those of their heterozygous and wild-type littermates (control, 95.1 ± 3.7 μm; *nrp2*$^{lacZ/lacZ}$, 129.1 ± 5.1 μm; $p < 0.0001$, Mann–Whitney U test). A similar dorsal spread and defasciculation of mDAN axons were observed when midbrain hemispheres were stained with an anti-β-gal antibody (*nrp2*$^{+/lacZ}$, n = 10 of 10; *nrp2*$^{lacZ/lacZ}$, n = 6 of 6) (supplemental Fig. 7, available at www.jneurosci.org as supplemental material). These data suggest that sema3F/nrp2 signaling defines the dorsal border of mDAN axon growth leading to the fasciculation of mDAN axons.

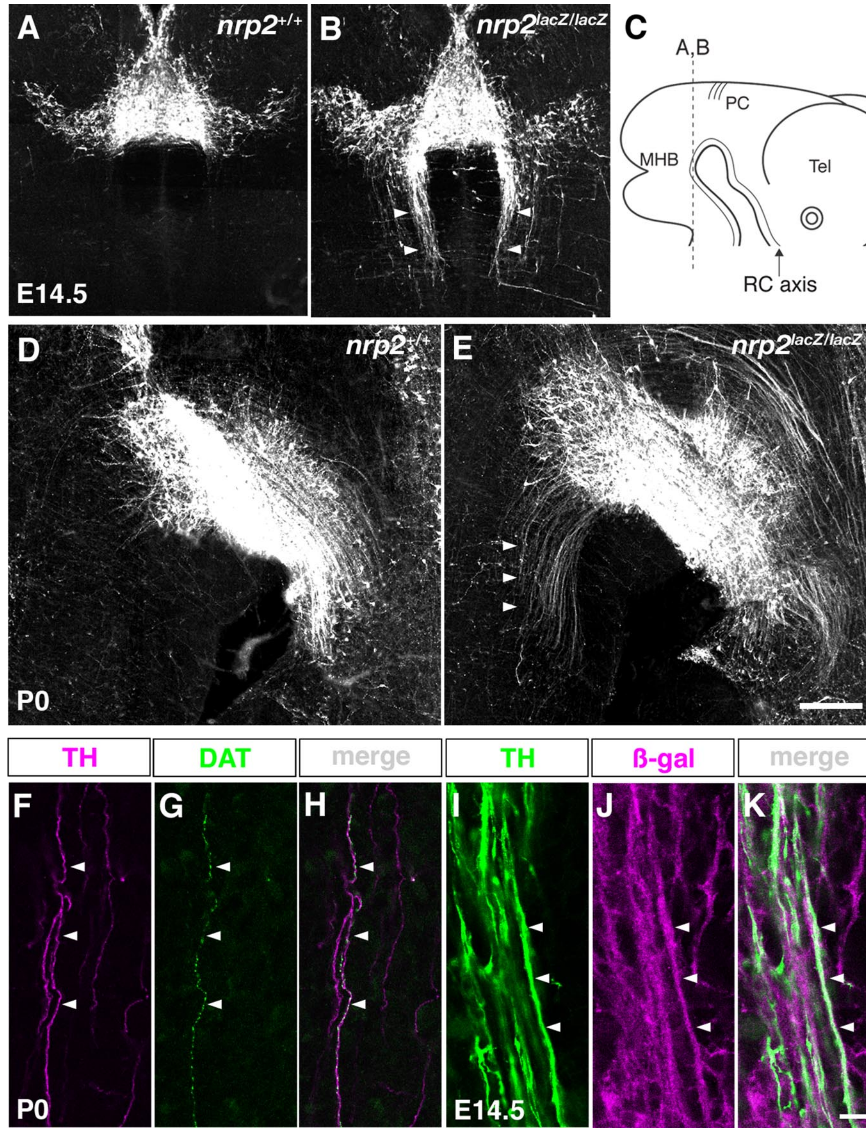

Figure 6. A subset of mDAN axons deflect in the caudal direction in *nrp2*-knock-out mice. ***A***, ***B***, TH immunostaining in coronal sections of wild-type (***A***) and *nrp2*-knock-out (***B***) mice at E14.5. Aberrant TH-positive fibers invaded the rostral hindbrain in an *nrp2*-knock-out mouse (***B,*** arrowheads). ***C***, Schematic representation showing the level of coronal sections in ***A*** and ***B***. Note that the RC axis curves in the midbrain. PC, Posterior commissure; Tel, telencephalon. ***D***, ***E***, TH immunostaining in parasagittal sections of *nrp2* $^{+/+}$ (***D***) and *nrp2*$^{lacZ/lacZ}$ (***E***) brains at P0. TH-positive fibers derived from the ventral midbrain, all of which were directed rostrally in a wild-type mouse (***D***), were deflected caudally in an *nrp2*-knock-out mouse (***E***, arrowheads). ***F–H***, Aberrant TH-positive fibers (magenta) immunostained for DAT (green). ***F***, ***G***, TH (***F***) and DAT (***G***) expression. ***H***, A merged view of ***F*** and ***G***. DAT was expressed on an aberrant TH-positive fiber (arrowheads). ***I–K***, Aberrant mDAN axons stained with antibodies against TH (green) and β-gal (magenta). ***I***, ***J***, TH (***I***) and β-gal (***J***) expression. ***K***, A merged view of ***I*** and ***J***. β-gal was expressed on aberrant mDAN axons (arrowheads). Scale bars: ***A***, ***B***, ***D***, ***E***, 200 μm; ***F–K***, 10 μm.

Discussion

FGF8 is a patterning molecule secreted from the MHB. We found misexpression of FGF8 disrupted the mDAN axonal trajectory and induced *sema3F* expression in the diencephalon/midbrain *in vitro*. Developmental expression of *Fgf8* at the MHB preceded *sema3F*, supporting that *sema3F* is also induced by FGF8 *in vivo*. *sema3F* was expressed in regions not occupied by mDAN axons and inhibited mDAN axon ourgrowth, suggesting that mDAN axons are guided by the growth-inhibitory activity of sema3F. Consistent with this, mDAN axons expressed a sema3F receptor, nrp2. Moreover, in *nrp2*-knock-out mice, some mDAN axons aberrantly extended caudally. These findings indicate that the MHB signaling center regulates the RC growth polarity of mDAN axons by inducing *sema3F* (Fig. 8*A*).

Disruption of mDAN axon trajectory by ectopic FGF8 expression

mDAN axonal trajectories were substantially perturbed by FGF8-beads (Fig. 1*B*). Although FGF8 acts as a guidance cue (Irving et al., 2002; Shirasaki et al., 2006), the fact that FGF8-beads did not repel mDAN axons (supplemental Fig. 8, available at www.jneurosci.org as supplemental material), together with a failure of MHB explants to repel mDAN axons (S. Nakamura et al., 2000), supports the view that FGF8 "indirectly" guides mDAN axons by inducing guidance molecules.

Some mDAN axons extended rostrally even after FGF8-bead implantation (Fig. 1*B*). This might be because some mDAN axons are insensitive to FGF8 signaling. This rostral growth can also be explained by assuming that early-extending mDAN axons have already passed the site of the bead before guidance molecules are induced. This is consistent with the findings that the rostral growth of mDAN axons initiates within 24 h after bead implantation (S. Nakamura et al., 2000), whereas alternations in gene expression by FGF8 requires 8–40 h (Liu and Joyner, 2001b).

FGF8 induced *sema3F*, which, in turn, guided mDAN axons (Fig. 8*A*). FGF8 and SHH collaborate to create the induction site for mDANs (Ye et al., 1998). Thus, FGF8 plays dual roles in mDAN development: induction and axon guidance.

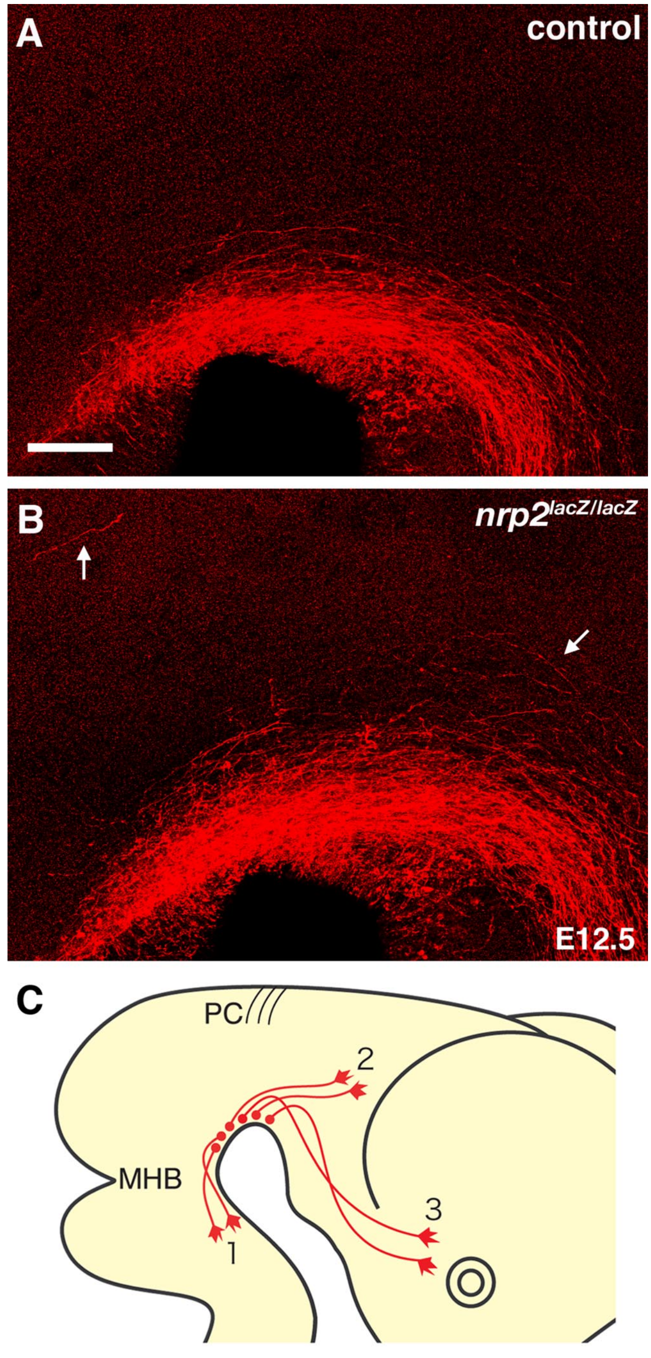

Figure 7. Dorsal spread of mDAN axons in *nrp2*-knock-out mice. ***A***, ***B***, TH immunostaining in flat-mount brain preparations of wild-type (***A***) and $nrp2^{lacZ/lacZ}$ (***B***) mice at E12.5. TH-positive fibers, which are relatively tightly fasciculated in a wild type (***A***), were defasciculated, with some deviating from their normal pathway in an *nrp2*-knock-out mouse (***B***, arrows). Scale bar, 200 μm. ***C***, Schematic diagram showing the trajectory of mDAN axons in *nrp2*-knock-out mice. In *nrp2*-knock-out mice, the trajectories of nrp2-positive mDAN axons were disrupted: a subset of axons grow caudally (1) and another part of them deflect dorsally (2). The remaining part projects normally (3). PC, Posterior commissure.

FGF8 induces *sema3F*

We found that exogenously applied FGF8 induced *sema3F* expression *in vitro*. FGF8 may also induce *sema3F* expression *in vivo* because (1) *Fgf8* expression at the MHB preceded *sema3F* and (2) SU5402, an FGF receptor tyrosine kinase inhibitor (Mohammadi et al., 1997), essentially abolished *sema3F* expression in the *otx2*-positive region *in vitro*. The findings that *sema3F* is expressed near *Fgf8*-expressing areas such as limb buds, kidneys, and brachial arches (Heikinheimo et al., 1994; Ohuchi et al., 1994; Crossley and Martin, 1995; Mahmood et al., 1995; Eckhardt and Meyerhans, 1998; Huber et al., 2005; Gammill et al., 2006) are consistent with our interpretation.

How does FGF8 induce *sema3F* expression? It seems unlikely that FGF8 signaling induces *sema3F* via Wnt signaling because *Wnt-1* electroporation failed to induce *sema3F* (supplemental Fig. 4*C*, available at www.jneurosci.org as supplemental material). Expression of *sema3F* in *Pea3*-expressing motor pools (Cohen et al., 2005) implies that FGF8 may induce *sema3F* via its general downstream target, *Pea3* (Raible and Brand, 2001; Roehl and Nüsslein-Volhard, 2001). Other potential candidates are the Sp family of transcription factors. *Sp8*, a member of the Sp family, is a downstream target of FGF8 in the telencephalon (Sahara et al., 2007). Human *sema3F* promoter does not contain a TATA-like box but rather putative Sp1 and Sp3 binding sites (Kusy et al., 2005). *Sp8* expression at the MHB (Bell et al., 2003; Treichel et al., 2003; Kawakami et al., 2004; Griesel et al., 2006) supports that Sp8 mediates *sema3F* induction by FGF8.

sema3F was not detected in the *Fgf8*-expressing region (Fig. 3*C*,*D*). This might be because *sema3F* is induced by FGF8 in a concentration-dependent manner. Indeed, dosage-dependent gene induction by FGF8 was reported recently (Storm et al., 2003, 2006; Badde and Schulte, 2008). Another possibility is that yet unidentified molecules that negatively regulate *sema3F* expression are activated in the *Fgf8*-expressing region. Additional studies are required to test these possibilities.

Contribution of sema3F/nrp2 signaling to mDAN axon guidance

Sema3F repelled mDAN axons, and a substantial population of these axons expressed nrp2. A similar repulsive effect *in vitro* was also reported recently (Hernández-Montiel et al., 2008). However, whether and how sema3F/nrp2 signaling contributes to mDAN axon guidance *in vivo* has remained unknown. Using genetic approaches, we have unraveled *in vivo* roles of sema3F/nrp2 signaling: (1) control of the RC growth polarity of mDAN axons; and (2) determination of the dorsal border of mDAN axon growth (Fig. 7*C*). We also found induction of *sema3F* by FGF8 as discussed above.

The caudally directed growth of mDAN axons in *nrp2*-knock-out mice demonstrates that nrp2 signaling regulates the RC polarity of mDAN axon growth. This guidance defect is not attributable to midbrain/hindbrain patterning defects because the expression of midbrain/hindbrain genes *otx2*, *en-2*, and *Fgf8*, appeared unaffected in *nrp2*-knock-out mice (supplemental Fig. 6, available at www.jneurosci.org as supplemental material). Nrp2 is an essential component not only for sema3F but also for sema3B and sema3C signaling (Chen et al., 1998; Giger et al., 1998; Takahashi et al., 1998), and *sema3C*, *sema3D*, and *sema3E* were expressed near mDAN axons (supplemental Fig. 3, available at www.jneurosci.org as supplemental material). However, sema3F is the most likely ligand to regulate the RC polarity of mDAN axon growth because (1) among class 3 semaphorins, only *sema3F* was detected at the MHB (Fig. 2*A*) (Chen et al., 2000; Giger et al., 2000; Watanabe et al., 2004), (2) sema3F inhibited mDAN axon outgrowth *in vitro* (Fig. 5*B*) (Hernández-Montiel et al., 2008), (3) axon guidance defects found in *sema3F*-null mice are almost phenotypically identical to those of *nrp2*-knock-out mice (Chen et al., 2000; Giger et al., 2000; Cloutier et al., 2002, 2004; Walz et al., 2002, 2007; Sahay et al., 2003; Huber et al., 2005), (4) sema3C affects mDAN axons as a chemoattractant (Hernández-Montiel et al., 2008), (5) sema3E does not bind to nrp2 (for review, see Kruger et al., 2005; Tran et al., 2007; Zhou et al., 2008), and (6) mDAN axon subsets extended rostrally, apparently ignoring the oculomotor nucleus where *sema3D* was highly expressed (supplemental Fig. 3*D*, available at www.jneurosci.org as supplemental material).

Because sema3F is a secreted protein, sema3F might repel mDAN axons by forming a caudal-high/rostral-low gradient. Indeed, the graded expression of guidance molecules regulates the RC axon guidance in other systems (Lyuksyutova et al., 2003; Bourikas et al., 2005; Liu et al., 2005; Zhu et al., 2006). However, isthmic explants does not chemorepel mDAN axons (S. Nakamura et al., 2000). Therefore, it is more likely that sema3F forms a local nonpermissive/repulsive territory, which would force mDAN axons to extend rostrally. The finding that sema3F transcripts and mDAN axons were distributed in a complementary manner supports this view.

The dorsally deflected growth of mDAN axons in *nrp2*-knock-out mice indicates that nrp2 signaling defines the dorsal border of mDAN axons. Our findings that mDAN axons extended immediately ventral to the *sema3F*-expressing region (Fig. 2*A*,*D*) and that sema3F inhibited mDAN axon outgrowth imply sema3F acts as a dorsal barrier to mDAN axons. Sema3C, which is expressed in the pretectum, attracts mDAN axons *in vitro* (Hernández-Montiel et al., 2008), whereas mDAN axons aberrantly invaded the pretectum in *nrp2*-knock-out mice (Fig. 7*A*,*B*). The discrepancy between the previous and these results might be attributable to the difference between *in vitro* and *in vivo* conditions.

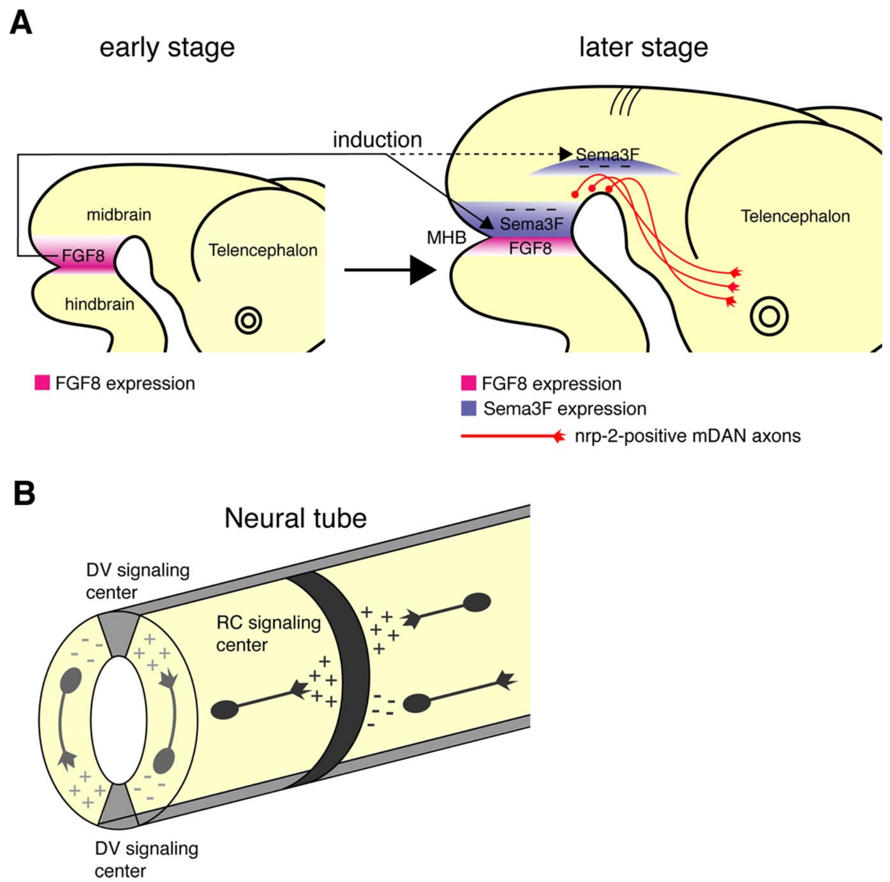

Figure 8. Summary diagram of the present study and model diagram of the regulation of axonal growth polarity by signaling centers. ***A***, Summary diagram showing the regulation of growth polarity of mDAN axons by FGF8 signaling. In early stages, MHB-derived FGF8 induces the *sema3F* expression at the MHB. Later, the axons of differentiated mDANs are guided rostrally by sema3F. Sema3F also provides the dorsal nonpermissive/repulsive territory to mDAN axons, defining the dorsal border of these axons. ***B***, Model diagram showing the roles of signaling centers in axon guidance along the DV and RC axes. Along the DV axis, the growth polarity of axons is regulated by the signaling centers controlling the DV polarization of the neural tube. In an analogous way, the signaling centers controlling the RC polarization of the neural tube are also involved in the growth polarity of axons along the RC axis.

Possible involvement of other molecules

FGF8 might also induce guidance molecules for mDAN axons other than *sema3F*. The fact that nrp2 was not detected in all mDAN axons, together with the finding that many mDAN axons still grew rostrally in *nrp2*-knock-out mice, raises the possibility that mechanisms other than sema3F/nrp2 signaling are involved. One candidate is ephrin-A/EphA signaling, which regulates the rostral turning of a hindbrain lateral commissural axon (Zhu et al., 2006). Moreover, FGF8 induces the expression of *ephrin-A*s (Shamim et al., 1999). However, mDAN axons grew rostrally even after the removal of glycosylphosphatidylinositol-anchored proteins (S. Mizushima and F. Murakami, unpublished observation). Wnts and SHH are other candidates. Gradients of these molecules regulate the RC axon guidance in the spinal cord (Lyuksyutova et al., 2003; Bourikas et al., 2005; Liu et al., 2005), and they are expressed in the ventral midbrain (Parr et al., 1993; Hynes et al., 1995a,b). Additional studies are required to test possible contributions by these molecules.

Roles of signaling centers in axon guidance along the RC and DV axes

The signaling centers controlling the DV polarization of the neural tube, the roof plate and the floor plate, play pivotal roles in axon guidance along the DV axis (for review, see Colamarino and Tessier-Lavigne, 1995; Murakami and Shirasaki, 1997). However, the role of signaling centers regulating the RC polarization in the RC axon guidance has remained unclear. Our results suggest that the RC polarity of mDAN axon growth is regulated by the MHB signaling center that governs the RC polarity of the midbrain/hindbrain (for review, see Liu and Joyner, 2001a; Wurst and Bally-Cuif, 2001; Raible and Brand, 2004; Nakamura et al., 2005). FGF8, a signaling molecule that can mimic MHB patterning activities, guides mDAN axons along the RC axis by inducing *sema3F* expression (Fig. 8*A*). A similar but somewhat different example can be found in commissural axon guidance. The floor plate is induced by a patterning molecule, SHH (for review, see Placzek and Briscoe, 2005). The induced floor plate secretes netrin-1. Netrin-1 in turn guides commissural axons ventrally (Kennedy et al., 1994; Serafini et al., 1994, 1996).

In addition to their indirect actions, patterning molecules controlling the DV polarization of the neural tube, BMPs and SHH, directly regulate the growth polarity of axons along the DV axis (Augsburger et al., 1999; Butler and Dodd, 2003; Charron et al., 2003). A growing body of evidence suggests that patterning molecules also directly regulate the axonal growth polarity along the RC axis (Lyuksyutova et al., 2003; Bourikas et al., 2005; Liu et al., 2005). It is interesting that the fundamental growth polarities of axons in the neural tube appear, in general, to be controlled by signaling centers, which are mediated by direct and indirect actions of pattering molecules (Fig. 8*B*).

References

Abeliovich A, Hammond R (2007) Midbrain dopamine neuron differentiation: factors and fates. Dev Biol 304:447–454.

Ang SL (2006) Transcriptional control of midbrain dopaminergic neuron development. Development 133:3499–3506.

Augsburger A, Schuchardt A, Hoskins S, Dodd J, Butler S (1999) BMPs as mediators of roof plate repulsion of commissural neurons. Neuron 24:127–141.

Badde A, Schulte D (2008) A role for receptor protein tyrosine phosphatase lambda in midbrain development. J Neurosci 28:6152–6164.

Bally-Cuif L, Alvarado-Mallart RM, Darnell DK, Wassef M (1992) Relationship between Wnt-1 and En-2 expression domains during early development of normal and ectopic met-mesencephalon. Development 115:999–1009.

Bell SM, Schreiner CM, Waclaw RR, Campbell K, Potter SS, Scott WJ (2003) Sp8 is crucial for limb outgrowth and neuropore closure. Proc Natl Acad Sci U S A 100:12195–12200.

Bourikas D, Pekarik V, Baeriswyl T, Grunditz A, Sadhu R, Nardo M, Stoeckli ET (2005) Sonic hedgehog guides commissural axons along the longitudinal axis of the spinal cord. Nat Neurosci 8:297–304.

Briscoe J, Ericson J (2001) Specification of neuronal fates in the ventral neural tube. Curr Opin Neurobiol 11:43–49.

Butler SJ, Dodd J (2003) A role for BMP heterodimers in roof plate-mediated repulsion of commissural axons. Neuron 38:389–401.

Caspary T, Anderson KV (2003) Patterning cell types in the dorsal spinal cord: what the mouse mutants say. Nat Rev Neurosci 4:289–297.

Charron F, Stein E, Jeong J, McMahon AP, Tessier-Lavigne M (2003) The morphogen sonic hedgehog is an axonal chemoattractant that collaborates with netrin-1 in midline axon guidance. Cell 113:11–23.

Chen H, Chédotal A, He Z, Goodman CS, Tessier-Lavigne M (1997) Neuropilin-2, a novel member of the neuropilin family, is a high affinity receptor for the semaphorins Sema E and Sema IV but not Sema III. Neuron 19:547–559.

Chen H, He Z, Bagri A, Tessier-Lavigne M (1998) Semaphorin-neuropilin interactions underlying sympathetic axon responses to class III semaphorins. Neuron 21:1283–1290.

Chen H, Bagri A, Zupicich JA, Zou Y, Stoeckli E, Pleasure SJ, Lowenstein DH, Skarnes WC, Chédotal A, Tessier-Lavigne M (2000) Neuropilin-2 regulates the development of selective cranial and sensory nerves and hippocampal mossy fiber projections. Neuron 25:43–56.

Chizhikov VV, Millen KJ (2005) Roof plate-dependent patterning of the vertebrate dorsal central nervous system. Dev Biol 277:287–295.

Ciliax BJ, Heilman C, Demchyshyn LL, Pristupa ZB, Ince E, Hersch SM, Niznik HB, Levey AI (1995) The dopamine transporter: immunochemical characterization and localization in brain. J Neurosci 15:1714–1723.

Cloutier JF, Giger RJ, Koentges G, Dulac C, Kolodkin AL, Ginty DD (2002) Neuropilin-2 mediates axonal fasciculation, zonal segregation, but not axonal convergence, of primary accessory olfactory neurons. Neuron 33:877–892.

Cloutier JF, Sahay A, Chang EC, Tessier-Lavigne M, Dulac C, Kolodkin AL, Ginty DD (2004) Differential requirements for semaphorin 3F and Slit-1 in axonal targeting, fasciculation, and segregation of olfactory sensory neuron projections. J Neurosci 24:9087–9096.

Cohen S, Funkelstein L, Livet J, Rougon G, Henderson CE, Castellani V, Mann F (2005) A semaphorin code defines subpopulations of spinal motor neurons during mouse development. Eur J Neurosci 21:1767–1776.

Colamarino SA, Tessier-Lavigne M (1995) The role of the floor plate in axon guidance. Annu Rev Neurosci 18:497–529.

Crossley PH, Martin GR (1995) The mouse Fgf8 gene encodes a family of polypeptides and is expressed in regions that direct outgrowth and patterning in the developing embryo. Development 121:439–451.

Crossley PH, Martinez S, Martin GR (1996) Midbrain development induced by FGF8 in the chick embryo. Nature 380:66–68.

Davis CA, Noble-Topham SE, Rossant J, Joyner AL (1988) Expression of the homeo box-containing gene En-2 delineates a specific region of the developing mouse brain. Genes Dev 2:361–371.

de Castro F, Hu L, Drabkin H, Sotelo C, Chédotal A (1999) Chemoattraction and chemorepulsion of olfactory bulb axons by different secreted semaphorins. J Neurosci 19:4428–4436.

Dickson BJ (2002) Molecular mechanisms of axon guidance. Science 298:1959–1964.

Dietrich S, Schubert FR, Lumsden A (1997) Control of dorsoventral pattern in the chick paraxial mesoderm. Development 124:3895–3908.

Eckhardt F, Meyerhans A (1998) Cloning and expression pattern of a murine semaphorin homologous to H-sema IV. Neuroreport 9:3975–3979.

Freed C, Revay R, Vaughan RA, Kriek E, Grant S, Uhl GR, Kuhar MJ (1995) Dopamine transporter immunoreactivity in rat brain. J Comp Neurol 359:340–349.

Fujisawa H (2004) Discovery of semaphorin receptors, neuropilin and plexin, and their functions in neural development. J Neurobiol 59:24–33.

Gammill LS, Gonzalez C, Bronner-Fraser M (2006) Neuropilin 2/semaphorin 3F signaling is essential for cranial neural crest migration and trigeminal ganglion condensation. J Neurobiol 67:47–56.

Giger RJ, Urquhart ER, Gillespie SKH, Levengood DV, Ginty DD, Kolodkin AL (1998) Neuropilin-2 is a receptor for semaphorin IV: insight into the structural basis of receptor function and specificity. Neuron 21:1079–1092.

Giger RJ, Cloutier JF, Sahay A, Prinjha RK, Levengood DV, Moore SE, Pickering S, Simmons D, Rastan S, Walsh FS, Kolodkin AL, Ginty DD, Geppert M (2000) Neuropilin-2 is required in vivo for selective axon guidance responses to secreted semaphorins. Neuron 25:29–41.

Gore BB, Wong KG, Tessier-Lavigne M (2008) Stem cell factor functions as an outgrowth-promoting factor to enable axon exit from the midline intermediate target. Neuron 2008 57:501–510.

Griesel G, Treichel D, Collombat P, Krull J, Zembrzycki A, van den Akker WM, Gruss P, Simeone A, Mansouri A (2006) Sp8 controls the anteroposterior patterning at the midbrain-hindbrain border. Development 133:1779–1787.

Hatanaka Y, Murakami F (2002) In vitro analysis of the origin, migratory behavior, and maturation of cortical pyramidal cells. J Comp Neurol 454:1–14.

Heikinheimo M, Lawshé A, Shackleford GM, Wilson DB, MacArthur CA (1994) Fgf-8 expression in the post-gastrulation mouse suggests roles in the development of the face, limbs and central nervous system. Mech Dev 48:129–138.

Hernández-Montiel HL, Tamariz E, Sandoval-Minero MT, Varela-Echavarría A (2008) Semaphorins 3A, 3C, and 3F in mesencephalic dopaminergic axon pathfinding. J Comp Neurol 506:387–397.

Huber AB, Kolodkin AL, Ginty DD, Cloutier JF (2003) Signaling at the growth cone: ligand-receptor complexes and the control of axon growth and guidance. Annu Rev Neurosci 26:509–563.

Huber AB, Kania A, Tran TS, Gu C, De Marco Garcia N, Lieberam I, Johnson D, Jessell TM, Ginty DD, Kolodkin AL (2005) Distinct roles for secreted semaphorin signaling in spinal motor axon guidance. Neuron 48:949–964.

Hynes M, Rosenthal A (1999) Specification of dopaminergic and serotonergic neurons in the vertebrate CNS. Curr Opin Neurobiol 9:26–36.

Hynes M, Poulsen K, Tessier-Lavigne M, Rosenthal A (1995a) Control of neuronal diversity by the floor plate: contact-mediated induction of midbrain dopaminergic neurons. Cell 80:95–101.

Hynes M, Porter JA, Chiang C, Chang D, Tessier-Lavigne M, Beachy PA, Rosenthal A (1995b) Induction of midbrain dopaminergic neurons by Sonic hedgehog. Neuron 15:35–44.

Irving C, Malhas A, Guthrie S, Mason I (2002) Establishing the trochlear motor axon trajectory: role of the isthmic organiser and Fgf8. Development 129:5389–5398.

Jessell TM (2000) Neuronal specification in the spinal cord: inductive signals and transcriptional codes. Nat Rev Genet 1:20–29.

Kawakami Y, Esteban CR, Matsui T, Rodríguez-León J, Kato S, Belmonte JC (2004) Sp8 and Sp9, two closely related buttonhead-like transcription factors, regulate Fgf8 expression and limb outgrowth in vertebrate embryos. Development 131:4763–4774.

Kennedy TE, Serafini T, de la Torre JR, Tessier-Lavigne M (1994) Netrins are diffusible chemotropic factors for commissural axons in the embryonic spinal cord. Cell 78:425–435.

Kolodkin AL, Levengood DV, Rowe EG, Tai YT, Giger RJ, Ginty DD (1997) Neuropilin is a semaphorin III receptor. Cell 90:753–762.

Kruger RP, Aurandt J, Guan KL (2005) Semaphorins command cells to move. Nat Rev Mol Cell Biol 6:789–800.

Kusy S, Potiron V, Zeng C, Franklin W, Brambilla E, Minna J, Drabkin HA, Roche J (2005) Promoter characterization of Semaphorin SEMA3F, a tumor suppressor gene. Biochim Biophys Acta 1730:66–76.

Lee KJ, Jessell TM (1999) The specification of dorsal cell fates in the vertebrate central nervous system. Annu Rev Neurosci 22:261–294.

Lindvall O, Björklund A (1983) Dopamine- and norepinephrine-containing neuron systems: their anatomy in the rat brain. In: Chemical neuroanatomy (Emson PC, ed), pp 229–255. New York: Raven.

Liu A, Joyner AL (2001a) Early anterior/posterior patterning of the midbrain and cerebellum. Annu Rev Neurosci 24:869–896.

Liu A, Joyner AL (2001b) EN and GBX2 play essential roles downstream of FGF8 in patterning the mouse mid/hindbrain region. Development 128:181–191.

Liu A, Losos K, Joyner AL (1999) FGF8 can activate Gbx2 and transform regions of the rostral mouse brain into a hindbrain fate. Development 126:4827–4838.

Liu Y, Shi J, Lu CC, Wang ZB, Lyuksyutova AI, Song X, Zou Y (2005) Ryk-mediated Wnt repulsion regulates posterior-directed growth of corticospinal tract. Nat Neurosci 8:1151–1159.

Lupo G, Harris WA, Lewis KE (2006) Mechanisms of ventral patterning in the vertebrate nervous system. Nat Rev Neurosci 7:103–114.

Lyuksyutova AI, Lu CC, Milanesio N, King LA. Guo N, Wang Y, Nathans J, Tessier-Lavigne M, Zou Y (2003) Anterior-posterior guidance of commissural axons by Wnt-frizzled signaling. Science 302:1984–1988.

Mahmood R, Bresnick J, Hornbruch A, Mahony C, Morton N, Colquhoun K, Martin P, Lumsden A, Dickson C, Mason I (1995) A role for FGF-8 in the initiation and maintenance of vertebrate limb bud outgrowth. Curr Biol 5:797–806.

Martinez S, Crossley PH, Cobos I, Rubenstein JL, Martin GR (1999) FGF8 induces formation of an ectopic isthmic organizer and isthmocerebellar development via a repressive effect on Otx2 expression. Development 126:1189–1200.

Mohammadi M, McMahon G, Sun L, Tang C, Hirth P, Yeh BK, Hubbard SR, Schlessinger J (1997) Structures of the tyrosine kinase domain of fibroblast growth factor receptor in complex with inhibitors. Science 276:955–960.

Murakami F, Shirasaki R (1997) Guidance of circumferentially growing axons by the floor plate in the vertebrate central nervous system. Cell Tissue Res 290:323–330.

Nakamura F, Kalb RG, Strittmatter SM (2000) Molecular basis of semaphorin-mediated axon guidance. J Neurobiol 44:219–229.

Nakamura H, Katahira T, Matsunaga E, Sato T (2005) Isthmus organizer for midbrain and hindbrain development. Brain Res Brain Res Rev 49:120–126.

Nakamura S, Ito Y, Shirasaki R, Murakami F (2000) Local directional cues control growth polarity of dopaminergic axons along the rostrocaudal axis. J Neurosci 20:4112–4119.

Niwa H, Yamamura K, Miyazaki J (1991) Efficient selection for high-expression transfectants with a novel eukaryotic vector. Gene 108:193–199.

Ohuchi H, Yoshioka H, Tanaka A, Kawakami Y, Nohno T, Noji S (1994) Involvement of androgen-induced growth factor (FGF-8) gene in mouse embryogenesis and morphogenesis. Biochem Biophys Res Commun 204:882–888.

Osumi N, Inoue T (2001) Gene transfer into cultured mammalian embryos by electroporation. Methods 24:35–42.

Parr BA, Shea MJ, Vassileva G, McMahon AP (1993) Mouse Wnt genes exhibit discrete domains of expression in the early embryonic CNS and limb buds. Development 119:247–261.

Placzek M, Briscoe J (2005) The floor plate: multiple cells, multiple signals. Nat Rev Neurosci 6:230–240.

Prakash N, Wurst W (2006) Genetic networks controlling the development of midbrain dopaminergic neurons. J Physiol 575:403–410.

Raible F, Brand M (2001) Tight transcriptional control of the ETS domain factors Erm and Pea3 by Fgf signaling during early zebrafish development. Mech Dev 107:105–117.

Raible F, Brand M (2004) Divide et Impera–the midbrain-hindbrain boundary and its organizer. Trends Neurosci 27:727–734.

Raper JA (2000) Semaphorins and their receptors in vertebrates and invertebrates. Curr Opin Neurobiol 10:88–94.

Roehl H, Nüsslein-Volhard C (2001) Zebrafish pea3 and erm are general targets of FGF8 signaling. Curr Biol 11:503–507.

Sahara S, Kawakami Y, Izpisua Belmonte JC, O'Leary DD (2007) Sp8 exhibits reciprocal induction with Fgf8 but has an opposing effect on anterior-posterior cortical area patterning. Neural Dev 2:10.

Sahay A, Molliver ME, Ginty DD, Kolodkin AL (2003) Semaphorin 3F is critical for development of limbic system circuitry and is required in neurons for selective CNS axon guidance events. J Neurosci 23:6671–6680.

Serafini T, Kennedy TE, Galko MJ, Mirzayan C, Jessell TM, Tessier-Lavigne M (1994) The netrins define a family of axon outgrowth-promoting proteins homologous to *C. elegans* UNC-6. Cell 78:409–424.

Serafini T, Colamarino SA, Leonardo ED, Wang H, Beddington R, Skarnes WC, Tessier-Lavigne M (1996) Netrin-1 is required for commissural axon guidance in the developing vertebrate nervous system. Cell 87:1001–1014.

Shamim H, Mahmood R, Logan C, Doherty P, Lumsden A, Mason I (1999) Sequential roles for Fgf4, En1 and Fgf8 in specification and regionalisation of the midbrain. Development 126:945–959.

Shirasaki R, Murakami F (2001) Crossing the floor plate triggers sharp turning of commissural axons. Dev Biol 236:99–108.

Shirasaki R, Tamada A, Katsumata R, Murakami F (1995) Guidance of cerebellofugal axons in the rat embryo: directed growth toward the floor plate and subsequent elongation along the longitudinal axis. Neuron 14:961–972.

Shirasaki R, Mirzayan C, Tessier-Lavigne M, Murakami F (1996) Guidance of circumferentially growing axons by netrin-dependent and -independent floor plate chemotropism in the vertebrate brain. Neuron 17:1079–1088.

Shirasaki R, Katsumata R, Murakami F (1998) Change in chemoattractant responsiveness of developing axons at an intermediate target. Science 279:105–107.

Shirasaki R, Lewcock JW, Lettieri K, Pfaff SL (2006) FGF as a target-derived chemoattractant for developing motor axons genetically programmed by the LIM code. Neuron 50:841–853.

Simeone A, Acampora D, Gulisano M, Stornaiuolo A, Boncinelli E (1992) Nested expression domains of four homeobox genes in developing rostral brain. Nature 358:687–690.

Simeone A, Acampora D, Mallamaci A, Stornaiuolo A, D'Apice MR, Nigro V, Boncinelli E (1993) A vertebrate gene related to orthodenticle contains a homeodomain of the bicoid class and demarcates anterior neuroectoderm in the gastrulating mouse embryo. EMBO J 12:2735–2747.

Smidt MP, Burbach JP (2007) How to make a mesodiencephalic dopaminergic neuron. Nat Rev Neurosci 8:21–32.

Storm EE, Rubenstein JL, Martin GR (2003) Dosage of Fgf8 determines whether cell survival is positively or negatively regulated in the developing forebrain. Proc Natl Acad Sci U S A 100:1757–1762.

Storm EE, Garel S, Borello U, Hebert JM, Martinez S, McConnell SK, Martin GR, Rubenstein JL (2006) Dose-dependent functions of Fgf8 in regulating telencephalic patterning centers. Development 133:1831–1844.

Takahashi T, Nakamura F, Jin Z, Kalb RG, Strittmatter SM (1998) Semaphorins A and E act as antagonists of neuropilin-1 and agonists of neuropilin-2 receptors. Nat Neurosci 6:487–493.

Takashima S, Kitakaze M, Asakura M, Asanuma H, Sanada S, Tashiro F, Niwa H, Miyazaki J, Hirota S, Kitamura Y, Kitsukawa T, Fujisawa H, Klagsbrun M, Hori M (2002) Targeting of both mouse neuropilin-1 and neuropilin-2 genes severely impairs developmental yolk sac and embryonic angiogenesis. Proc Natl Acad Sci U S A 99:3657–3662.

Tamada A, Kumada T, Zhu Y, Matsumoto T, Hatanaka Y, Muguruma K, Chen Z, Tanabe Y, Torigoe M, Yamauchi K, Oyama H, Nishida K, Murakami F (2008) Crucial roles of Robo proteins in midline crossing of cerebellofugal axons and lack of their up-regulation after midline crossing. Neural Dev 3:29.

Tanabe Y, Jessell TM (1996) Diversity and pattern in the developing spinal cord. Science 274:1115–1123.

Tanaka A, Miyamoto K, Minamino N, Takeda M, Sato B, Matsuo H, Matsumoto K (1992) Cloning and characterization of an androgen-induced growth factor essential for the androgen-dependent growth of mouse mammary carcinoma cells. Proc Natl Acad Sci U S A 89:8928–8932.

Tessier-Lavigne M, Goodman CS (1996) The molecular biology of axon guidance. Science 274:1123–1133.

Tran TS, Kolodkin AL, Bharadwaj R (2007) Semaphorin regulation of cellular morphology. Annu Rev Cell Dev Biol 23:263–292.

Treichel D, Schöck F, Jäckle H, Gruss P, Mansouri A (2003) mBtd is required to maintain signaling during murine limb development. Genes Dev 17:2630–2635.

Walz A, Rodriguez I, Mombaerts P (2002) Aberrant sensory innervation of the olfactory bulb in neuropilin-2 mutant mice. J Neurosci 22:4025–4035.

Walz A, Feinstein P, Khan M, Mombaerts P (2007) Axonal wiring of guanylate cyclase-D-expressing olfactory neurons is dependent on neuropilin 2 and semaphorin 3F. Development 134:4063–4072.

Wang LC, Rachel RA, Marcus RC, Mason CA (1996) Chemosuppression of retinal axon growth by the mouse optic chiasm. Neuron 17:849–862.

Watanabe Y, Toyoda R, Nakamura H (2004) Navigation of trochlear motor axons along the midbrain-hindbrain boundary by neuropilin 2. Development 131:681–692.

Wurst W, Bally-Cuif L (2001) Neural plate patterning: upstream and downstream of the isthmic organizer. Nat Rev Neurosci 2:99–108.

Yamauchi K, Mizushima S, Muguruma K, Tamada A, Takashima S, Murakami F (2004) Fgf8-induced Sema3F is involved in axon guidance of the midbrain dopaminergic neurons. Neurosci Res 50:S167.

Yamauchi K, Mizushima S, Tamada A, Yamamoto N, Takashima S, Murakami F (2007) FGF8-induced Semaphorin 3F regulates growth polarity of midbrain dopaminergic axons. Neurosci Res 58:S50.

Ye W, Shimamura K, Rubenstein JL, Hynes MA, Rosenthal A (1998) FGF and Shh signals control dopaminergic and serotonergic cell fate in the anterior neural plate. Cell 93:755–766.

Yu TW, Bargmann CI (2001) Dynamic regulation of axon guidance. Nat Neurosci 4:1169–1176.

Zhou Y, Gunput RA, Pasterkamp RJ (2008) Semaphorin signaling: progress made and promises ahead. Trends Biochem Sci 33:161–170.

Zhu Y, Guthrie S, Murakami F (2006) Ephrin A/EphA controls the rostral turning polarity of a lateral commissural tract in chick hindbrain. Development 133:3837–3846.

Zou Y, Stoeckli E, Chen H, Tessier-Lavigne M (2000) Squeezing axons out of the gray matter: a role for slit and semaphorin proteins from midline and ventral spinal cord. Cell 102:363–375.